Published in final edited form as:

Genesis. 2021 June ; 59(5-6): e23418. doi:10.1002/dvg.23418.

Altering metabolite distribution at *Xenopus* cleavage stages affects left-right gene expression asymmetries

Rosemary M. Onjiko[2], **Peter Nemes**[1,2,3], **Sally A. Moody**[1,*]

[1]Department of Anatomy and Cell Biology, The George Washington University School of Medicine and Health Sciences, Washington DC, USA

[2]Department of Chemistry, The George Washington University, Washington DC, USA

[3]Department of Chemistry & Biochemistry, University of Maryland, College Park, College Park MD, USA

Abstract

The left-right (L-R) axis of most bilateral animals is established during gastrulation when a transient ciliated structure creates a directional flow of signaling molecules that establish asymmetric gene expression in the lateral plate mesoderm. However, in some animals, an earlier differential distribution of molecules and cell division patterns initiate or at least influence L-R patterning. Using single-cell high-resolution mass spectrometry, we previously reported a limited number of small molecule (metabolite) concentration differences between left and right dorsal-animal blastomeres of the 8-cell *Xenopus* embryo. Herein, we examined whether altering the distribution of some of these molecules influenced early events in L-R patterning. Using lineage tracing, we found that injecting right-enriched metabolites into the left cell caused its descendant cells to disperse in patterns that varied from those in control gastrulae; this did not occur when left-enriched metabolites were injected into the right cell. At later stages, injecting left-enriched metabolites into the right cell perturbed the expression of genes known to: 1) be required for the formation of the gastrocoel roof plate (*foxj1*); 2) lead to the asymmetric expression of Nodal (*dand5/coco*); or 3) result from asymmetrical *nodal* expression (*pitx2*). Despite these perturbations in gene expression, we did not observe heterotaxy in heart or gut looping at tadpole stages. These studies indicate that altering metabolite distribution at cleavage stages at the concentrations tested in this study impacts the earliest steps of L-R gene expression that then can be compensated for during organogenesis.

Keywords

dand5 ; *coco* ; *pitx2* ; *foxj1* ; gastrocoel roof plate; *Xenopus*

[*]Corresponding author: Dr. Sally A. Moody, Department of Anatomy and Cell Biology, The George Washington University School of Medicine and Health Sciences, 2300 I (capital eye) Street, N.W., Washington DC, 20037, USA, 1-202-994-2878 (voice); 1-202-994-8885 (fax), samoody@gwu.edu.

INTRODUCTION

Establishing the three cardinal axes of the chordate embryo – anterior-posterior (A-P), dorsal-ventral (D-V), and left-right (L-R) – is an early and essential aspect of development. Numerous studies have identified differentially inherited maternal molecules that play key roles in initiating the A-P and D-V axes in several animals, including *Xenopus* (Davidson, 1990; Heasman, 2006; Houston, 2012; King et al., 2005). However, the L-R axis appears to be initiated in most vertebrates during gastrulation with the formation of a transient, motile cilia-bearing organ (gastrocoel roof plate [GRP] in *Xenopus*, node in mouse, Kupffer's vesicle in fish) that creates a directional flow of signaling molecules to initiate asymmetric *Nodal* gene expression in the lateral plate mesoderm, leading to asymmetries in organ looping and placement in the body cavity (Blum et al., 2014; Blum and Ott, 2018; Courtelis et al., 2014; Namigai et al., 2014). In some invertebrates, however, L-R asymmetries are established at cleavage stages by the orientation of early cell divisions (Chou et al., 2016; Kuroda et al., 2009; Courtelis et al., 2014). Even in *Xenopus*, there is some evidence for molecular and/or cell division L-R asymmetries prior to the establishment of the GRP (Adams et al., 2006; Bunney et al., 2003; Danilchik et al., 2006; Hyatt and Yost, 1998).

Single-cell high-resolution mass spectrometry (HRMS) is a recent technological development to quantify metabolic differences between cells in an unbiased manner. It has been critical for revealing numerous roles for metabolites in several aspects of animal and plant development (Krejci and Tennessen, 2017). Previously we dissected single left and right dorsal-animal blastomeres from the 8-cell *Xenopus laevis* embryo, and used capillary electrophoresis (CE) HRMS coupled with multi-solvent extraction to uncover small molecule (metabolite) differences between left and right blastomeres (Onjiko et al., 2016). Although most metabolites were comparably produced in the left dorsal-animal (L-D1) versus right dorsal-animal (R-D1) cell, we detected 10 distinct metabolites that accumulated differently: leucine, isoleucine, ethanolamine, GABA, and trolamine were enriched in L-D1, whereas creatine, acetylcarnitine, spermidine, S-adenosylmethionine, and putrescine were more abundant in R-D1. Mapping these differentially enriched metabolites against known metabolic pathways suggested that the arginine-proline metabolic pathway is enriched in R-D1. The biological significance of these L-R metabolite asymmetries, however, remained elusive.

To address this knowledge gap, herein we assessed whether this early left-right difference in metabolite distribution at cleavage stages has an impact on the development of L-R gene expression and/or organ placement during *Xenopus* embryogenesis. This was accomplished by microinjecting cocktails of left-enriched metabolites into R-D1 and right-enriched metabolites into L-D1. Using lineage tracing to identify the cells descended from the midline daughter of the injected blastomere, we found that injecting right-enriched metabolites into L-D1 caused its descendant cells to disperse in patterns that subtly varied from those in control gastrulae; this did not occur when left-enriched metabolites were injected into the right cell. When examined at later stages, embryos in which R-D1 was injected with left-enriched metabolites at the 8-cell stage showed perturbed expression of genes known to: 1) be required for the formation of the GRP (*foxi1*), 2) lead to the asymmetric expression of Nodal (*dand5/coco*) or 3) result from asymmetrical *nodal*

expression (*pitx2*). Despite these perturbations in gene expression, we did not observe heterotaxy in heart or gut looping at tadpole stages, indicating that the impact of altering the distribution of the tested metabolites at cleavage stages at the concentrations tested in this study is confined to the earliest steps of the process and can be compensated for by later molecular interactions during organogenesis.

METHODS

Obtaining embryos and microinjections:

Fertilized *Xenopus laevis* embryos were obtained by natural mating (Moody, 2018), and chosen at the 2-cell stage to accurately identify the dorsal and ventral animal blastomeres at later stages (Klein, 1987; Miyata et al., 1987; Moody, 2018). When selected embryos reached 8-cells, the left (L-D1) or right (R-D1) dorsal-animal blastomere (Fig. 1A; nomenclature of Hirose and Jacobson, 1979) was microinjected with a metabolite cocktail according to standard methods (Moody, 2018). For embryos used for lineage tracing experiments, after the 8-cell metabolite-cocktail injection the 16-cell, the midline descendant of the injected cell (L-D11 or R-D11; nomenclature of Hirose and Jacobson, 1979) was microinjected with 1 nL of 1% fluorescein dextran amine (FDA; ThermoFisher) (Fig. 1B). Only the midline descendant was analyzed because it had the potential to reveal movement of the clone to the opposite side of the embryo. As controls, sibling embryos were injected only with lineage tracer. Embryos were cultured in a series of diluted Steinberg's solution until fixation. Embryos for each assay were derived from a minimum of three different sets of outbred parents.

Metabolite cocktails:

Previously, we found that creatine, acetylcarnitine, spermidine, S-adenosylmethionine, and putrescine were enriched in right versus left D1 blastomeres (approx. 2.6-, 1.8-, 28.9-, 1.7-, 2.1-fold, respectively), whereas leucine, isoleucine, ethanolamine, GABA, and trolamine were enriched in left versus right D1 blastomeres (approx. 2.4-, 2.1-, 1.5-, 3.0-, 2.0-fold, respectively) (Onjiko et al., 2016). To test whether these endogenous differences may have a biological relevance to L-R patterning, we selected 3 metabolites from each group by considering relative abundance, endogenous concentration, and compound availability and stability. A cocktail of three of the left-enriched metabolites containing leucine, isoleucine, and GABA (mixture "Lmet") was microinjected into the right dorsal-animal blastomere (R-D1) and a cocktail of three of the right-enriched metabolites containing creatine, acetylcarnitine, and S-adenosylmethionine (mixture "Rmet") was microinjected into the left dorsal-animal blastomere (L-D1). Although precise quantification of endogenous metabolites can be technically challenging in these cells due to rapid embryonic development, alternating cell cycles, and known metabolic variability between embryos, even within the same batch (Vastag et al., 2011), our previous experiments provided useful guidance to design this portion of the study. For each metabolite, we estimated the endogenous concentrations based on external concentration calibration, as previously described (Onjiko et al., 2015). To account for biological variability, estimated concentration are reported as follows: leucine (100 pmol), isoleucine (100 pmol), GABA (10 pmol), S-adenosylmethionine (10 pmol), creatine (200 pmol), and acetylcarnitine (10

pmol). Since embryos from the same clutch of embryos can contain varying amounts of metabolites (Vastag et al., 2011), the study also included injections delivering double metabolite amounts, with the understanding that precise levels of the metabolites are expected to vary between embryos.

Lineage tracing:

FDA-injected embryos were raised to early neural plate stages (13-14, Nieuwkoop and Faber, 1994), fixed in 4% phosphate-buffered paraformaldehyde and stored at 4° C in phosphate-buffered saline. Fluorescent clones were photographed using an epifluorescence stereomicroscope; the resulting images were blinded to manipulation and categorized independently by two authors for the type of clone. The width of the clone from the midline was measured with a grid at 10X: type A clones were ≤2 grid squares at its widest point; type B clones were 2.0-2.5 squares; type C clones were 2.5-3.0 squares; type D clones were >3.0 squares; type E clones did not reach the blastopore. Frequencies of each type were compared between manipulations by the Chi-square test ($p < 0.05$ considered significant).

In situ hybridization (ISH):

To determine if altering the metabolite concentration affected the expression of genes involved in the early steps of L-R patterning, embryos were microinjected with metabolite cocktails as above, raised to appropriate stages for expression of: *foxj1* (stage 10.5; Stubbs et al., 2008), *dand5/coco* (stage 16-18; Vonica and Brivanlou, 2007), or *pitx2* (stage 30-32; Ryan et al., 1998), then fixed and processed for ISH as previously described (Yan et al., 2009). Antisense, DIG-labeled RNA probes for each gene were synthesized *in vitro* by standard methods (MEGAscript kit; Ambion). Samples were blinded to the manipulation and gene expression patterns on the left versus right sides were analyzed independently by two authors. For *foxj1* expression, each author independently used a video camera attached to a stereomicroscope and Olympus CellSense software, to mark the midpoint of the blastopore, draw a line from that point to the animal pole, and measure the length of the *foxj1* domain at 10X from that line on the right and left side with an eyepiece reticule (Fig. 3). Based on classical fate maps (Keller, 1975) the midpoint of blastopore line is presumed to represent the dorsal midline. The lengths averaged from the two authors were compared for significance between injected and control sides by a two-tailed, paired Wilcoxon test and between experimental and control groups by a two-tailed, unpaired Mann-Whitney test ($p < 0.05$ considered significant). For *dand5* expression, after ISH was completed, the embryo was dissected to expose the GRP. The left and right expression domains were scored independently by two authors as being larger/longer/darker on the right side, on the left side, equal on both sides, or absent on both sides (Fig. 4). For *pitx2* expression, embryos were scored independently by two authors for expression in the lateral plate mesoderm on the left side, right side, or both sides. The frequencies of gene expression patterns for *dand5* and *pitx2* between experimental and control groups were assessed for significance by the Chi-square test ($p<0.05$ considered significant).

Analysis of heterotaxy:

Embryos were microinjected as above and raised to tadpole stages. Tadpoles were fixed, samples were blinded to the manipulation, and the direction of heart looping and gut

coiling independently assessed by two authors using standard criteria (Hyatt and Yost, 1998; Sempou et al., 2018).

RESULTS

To assess whether the metabolites that we previously reported to be enriched in the left or right dorsal-animal blastomeres of the 8-cell *Xenopus* embryo (Onjiko et al., 2016) influence early aspects of L-R asymmetry in the embryo, we injected a cocktail of left-enriched metabolites (cocktail "Lmet" containing leucine, isoleucine, and GABA) into the right dorsal-animal blastomere (R-D1) or injected a cocktail of right-enriched metabolites (cocktail "Rmet" containing S-adenosylmethioine, creatine, and acetylcreatine) into the left dorsal-animal blastomere (L-D1) (Fig. 1A). Since previous work demonstrated that altering the distribution of dorsal-enriched and ventral-enriched metabolites alter the post-gastrula distribution of blastomere clones (Onjiko et al., 2015), we first assessed whether perturbing the left-right (L-R) metabolite asymmetry at the 8-cell stage altered the distribution of clones in the neural ectoderm, a major derivation of these blastomeres (Moody and Kline, 1990). First, the metabolite cocktail was injected at the 8-cell stage, and when the cell divided, a fluorescent lineage tracer (FDA) was injected into the dorsal midline 16-cell daughter (Fig. 1B). This descendant cell was chosen for analysis because previous fate mapping revealed that its clone approximates the midline of the neural plate (Moody, 1987); therefore, changes in cell dispersal would be readily detected. We classified the distribution of descendant cells in the neural ectoderm in control embryos that were injected only with FDA-lineage tracer (i.e., without added metabolites) in four patterns that ranged from a narrow strip of cells extending along the anterior-posterior axis from the animal pole to the closing blastopore (type A), to types in which cells extended progressively more laterally (types B - D) (Fig. 2A). Control clones of the R-D11 blastomere were primarily types A and C, and those of the L-D11 blastomere were primarily a mixture of types A, C, and D (Fig. 2B); the differences in distribution between control R-D11 and L-D11 clones were not significant ($p > 0.05$, Chi-square test), indicating there is no inherent L-R asymmetry in D11 clone distribution. The distribution of Lmet-injected R-D11 clones was indistinguishable from R-D11 controls ($p>0.05$), indicating no effect of the injected metabolites on clone dispersal patterns. In contrast, Rmet-injected L-D11 clones were distributed significantly differently compared to control L-D11 clones ($p < 0.001$); these embryos had fewer type A and D type clones and more type B clones. About 10% of embryos showed a unique pattern of compact anterior clones that did not extend to the posterior located blastopore (type E) (Fig. 2A, B). The cells in type E clones were the same size as unlabeled cells on the control side of the same embryo, suggesting that convergence-extension rather than cell cycle was perturbed. These data indicate that the distribution of the cells just after gastrulation that are derived from a left dorsal-animal blastomere is subtly sensitive to altered cleavage-stage metabolite distribution.

We next perturbed the metabolite distribution asymmetry at the 8-cell stage and monitored gene expression patterns in the precursor cells of the GRP, a transient organ in the roof of the posterior gut that functions to establish L-R asymmetry in the *Xenopus* embryonic lateral plate mesoderm (Blum and Ott, 2018). It should be noted that blastomeres R-D1 and L-D1 are major contributors to the archenteron roof (Moody and Kline, 1990), and

more precise fate-mapping of the *foxj1*-expressing cells reveals that 4-cell stage dorsal blastomeres contribute to the central regions of the GRP (Vick et al., 2009; Tingler et al., 2014). Foxj1 is a forkhead transcription factor that is required for the formation of cilia in the GRP and is expressed by GRP precursors in the supra-blastoporal mesoderm of the early gastrula (Stubbs et al., 2008; Tingler et al., 2014). To analyze each embryo, we identified the center of the pigmented blastopore ingression site, which according to fate maps is a good representation of the dorsal midline (Keller, 1975), and then measured the length of the *foxj1* domain on the left versus right side with an eyepiece reticule. In control, uninjected embryos the length of the *foxj1* domain was comparable on left and right sides (Fig. 3A, C; $p > 0.05$). The lengths on left and right sides also were indistinguishable in Rmet-injected L-D1 embryos (Fig. 3C; $p > 0.05$). In Lmet-injected R-D1 embryos, however, the right domain of *foxj1*, descended from the metabolite cocktail-injected side of the embryo, was significantly longer than the left domain (Fig. 3B, C; $p < 0.005$). When lengths were compared between Lmet-injected R-D1 embryos and control embryos, the left domain was significantly shorter and the right domain was significantly longer ($p < 0.0005$). Another difference that we observed was that in some embryos there was no detectable *foxj1* expression at these stages: 5.3% in controls (n = 76), 25% in Rmet-L-D1 (n = 48) and 25% in Lmet-R-D1 (n = 28). These frequencies of presumed repression or delay in *foxj1* expression were significantly different between metabolite cocktail-injected and control embryos ($p < 0.01$, Chi-square test). Together, these results show that altering metabolite asymmetry in the 8-cell stage precursors of the archenteron roof, by either type of injection, significantly perturbed the normal pattern of *foxj1* expression prior to the formation of the GRP.

We next assessed the expression of *dand5*, whose protein is essential for establishing L-R asymmetry by inhibiting Nodal signaling in the right lateral mesoderm (Vonica and Brivanlou, 2007; Schweickert et al., 2010). Consistent with these previous reports, in our control, uninjected siblings, *dand5* expression was larger, longer or darker primarily in the right GRP (Fig. 4Aa, Fig. 4B); in a minority of cases, it was more strongly expressed on the left side (Fig. 4Ab), equal on both sides (Fig. 4Ac), or undetectable (Fig. 4Ad; Fig. 4B). Because *dand5* is only required on the right side of the GRP (Vonica and Brivanlou, 2007), we only tested whether injection of Lmet into R-D1 perturbed its expression pattern. In these embryos, *dand5* was expressed more strongly on the right side in only a small percentage of embryos, and instead it was predominantly undetectable on both sides (Fig. 4B, 4C; $p < 0.00001$, Chi-square test). A similar bilateral loss of *dand5* previously was reported when embryos were depleted of *fgfr4* (Sempou et al., 2018), indicating it is a biological phenotype and not a failure of the assay; in addition, control and experimental samples were processed in parallel to avoid such an artifact. We next assessed whether the perturbations of *dand5* expression in the GRP led to a similar asymmetry in gene expression in the lateral plate mesoderm. As previously reported (Ryan et al., 1998), *pitx2* was asymmetrically expressed in the left lateral plate mesoderm in nearly every control embryo; Rmet-injected L-D1 embryos showed the same frequency (Fig. 5A, B; $p > 0.05$, Chi-square test). In contrast, in Lmet-injected R-D1 embryos *pitx2* expression often was bilateral (Fig. 5B; $p < 0.005$); there were no Lmet-injected R-D1 embryos in which *pitx2* expression was only in the right lateral plate mesoderm. Together these assays demonstrate that altering the distribution

of metabolites at cleavage stages perturbed gene expression asymmetry in both the GRP and lateral plate mesoderm. However, this change in gene expression did not ultimately result in reversals in heart looping or gut coiling directions at tadpole stages: both were predominantly normal (heart, 21/22; gut, 20/22).

DISCUSSION

It is well-established that in most bilateral animals the L-R axis is effectively established during gastrulation primarily by a transient organ with motile cilia that create a leftward flow of signaling molecules that establishes asymmetric Nodal signaling and gene expression in the lateral plate mesoderm (Blum et al., 2014; Blum and Ott, 2018; Courtelis et al., 2014; Namigai et al., 2014). However, the L-R axis of some animals is established by alternate processes. For example, neither *Drosophila* nor *C. elegans* utilize Nodal signaling, and in some snails asymmetric Nodal signaling is established during cleavage stages as the result of asymmetric, spiral cleavages during the third cell division (reviewed in Blum and Ott, 2018). *In C. elegans*, chiral cortical actomyosin flow is required for chirality of cleavage planes that break L-R symmetry (Courtelis et al., 2014). Interestingly, in *Xenopus*, in which the GRP is firmly established as regulating L-R gene expression and organ L-R asymmetries, there also is evidence for chirality of the early cleavage divisions. Danilchik et al. (2006) observed a counterclockwise torsion between the left and right blastomeres during the first cleavage of normal embryos, demonstrating an inherently chiral cleavage pattern. Treatment of fertilized eggs at the 1-cell stage – but not later – with butanedione monoxide, an inhibitor of ATPase-sensitive K^+ and Ca^{2+} channels also reported to disrupt actin filament assembly, exaggerated this chirality and resulted in tadpole heart and gut L-R heterotaxy. These authors suggested that the cortical cytoskeleton of the egg has an endogenous vectoral orientation that may localize maternal factors to one side of the embryo. Based on these studies in nematode and frog, and the observation that the actin-related *diaphanous* gene in the pond snail is the likely locus regulating handedness (Kuroda et al., 2016), it has been proposed that cytoskeletal asymmetries in the egg may have been an ancestral source of laterality, upon which the cilia-based organs were later built (Blum and Ott, 2018; Namigai et al., 2014; Vandenberg et al., 2013).

It is well documented in *Xenopus* that asymmetries in maternal mRNAs play important roles in animal-vegetal (approximating A-P) and D-V axis formation (Heasman, 2006; King et al., 2005; Houston, 2012). High resolution, single cell RNA-seq analyses confirmed several animal-vegetal differences, but did not detect significant mRNA differences between left and right 8-cell *Xenopus* blastomeres (De Domenico et al., 2015). Nonetheless, there are a few reports of L-R protein asymmetries at cleavage stages. For example, 14-3-3E protein is sequestered to the right cell at the 2 cell-stage (Bunney et al., 2003), and H^+-V-ATPase subunit A protein is more abundant in one of the 2 cell blastomeres (presumed right side but not demonstrated; Adams et al., 2006); both proteins are reported to be required for normal L-R patterning. In another report, although the *Vg1* maternal transcript is found in all vegetal cells, experimentally introducing signaling-competent Vg1 protein, showed that increasing Vg1 in right side, but not left side, vegetal blastomeres, caused L-R reversals and randomized heart looping and gut coiling (Hyatt and Yost, 1998). Zic3 has been proposed to carry out the effects of right-sided Vg1 signaling (Kitaguchi et al., 2000). Both studies

suggest that right side-specific translation of endogenous *Vg1* and *Zic3* contribute to L-R axis formation upstream of Nodal.

Our previous work examined small molecule (viz. metabolic, not mRNA, not protein) differences between single 8-cell blastomeres, and demonstrated quantitative differences between left and right blastomeres (Onjiko et al., 2016). Herein, we tested the functional consequences of these differences, and demonstrate that a cocktail of the most abundantly different metabolites can have subtle but significant effects on clone dispersal and the expression of a few genes involved in early aspects of L-R axis formation. First, injection of right-enriched metabolites into the left dorsal-animal blastomere caused the clone of its midline 16-cell daughter to disperse in subtly different patterns at stages just after the completion of gastrulation. We previously reported that gastrulation movements were significantly altered when ventral-enriched metabolites were introduced into 16-cell dorsal blastomeres and vice versa, causing cells to end up in different tissues (Onjiko et al., 2015). However, we did not observe such a dramatic effect with L-R metabolites, perhaps because there is no notable L-R difference in clone distribution in control embryos or the more lateral sister blastomere that we did not test was affected. It also is possible that the subtle disturbance we report may not be related to the metabolites altering cell fate, but to causing a minor, temporary delay in cleavage furrow closure that allowed lineage tracer to expand into the more lateral sister blastomere. Nonetheless, it is interesting that we only observed an effect when L-D1 was perturbed; this is consistent with the proposal that there is a cleavage stage L-R “coordination center” located on the left side (Hyatt and Yost, 1998). Because a lineage study of different regions of the tadpole heart showed laterality differences in blastomere origins that were significantly disrupted in tadpoles displaying cardiac heterotaxia (Ramsdell et al., 2006), it would be worth investigating whether changes in metabolite distribution that interfere with clone distribution also perturb contributions to the GRP and/or heart.

We also observed gene expression differences in *foxj1*, *dand5*, and *pitx2* but only when left-enriched metabolites were injected into the right dorsal-animal blastomere. This finding is consistent with previous studies that show proteins involved in heterotaxy being localized to right side blastomeres (Bunney et al., 2003; Adams et al., 2006; Tingler et al., 2014), and correlates with the observation that flow at the GRP is required only from right to left sides (Vick et al., 2009; Blum and Ott, 2018). Hyatt and Yost (1998) posited that experimentally manipulating the right side of the cleavage embryo, as we did, interferes with the left side-located L-R coordination center. Perhaps this explains why the expression of *foxj1* was attenuated on the left side of right-side injected embryos in our study. This could be investigated by injecting Lmet metabolites into the R-V1 cell. While it would be interesting to investigate this possibility, unlike these previous studies, we did not observe heterotaxy in tadpoles. This implies that the metabolic imbalances we caused at cleavage stages have only transient effects on gene expression that can be compensated for by a robust GRP system that restores laterality in tadpole organs. Alternatively, injection of Lmet into R-D1 may shift the dorsal midline to the right, maintaining symmetry in *foxj1* expression. In addition, injecting higher metabolite concentrations or metabolites other than those tested here may promote more pronounced effects on L-R patterning of the embryo that translate into the tadpole stages.

Remaining questions are what happens at the cellular level in a blastomere when a different set of small molecules is introduced: are the effects due to the introduced metabolites or to dilution of the cell's endogenous complement of metabolites? It also will be important to test whether increasing the endogenous metabolites affect cell fate and/or gene expression. Injected metabolites, by virtue of their charge, could alter the normal flow of molecules through gap junctional complexes that are known to be active during cleavage stages (Warner et al., 1984; Adams et al., 2006; Cofre and Abdelhay, 2007). It is plausible that changes in metabolite distribution alter cytoskeletal organization, which could affect cell movements and/or cell division rates or orientation. Changes in metabolite distribution also could perturb the normal availability of amino acids for local protein synthesis. These in turn could affect every aspect of an early cell's life including signaling to its neighbors and responding to signals from its neighbors. It would be most helpful to determine in what cellular compartment the metabolite differences reside. For example, yolk proteins account for about 90% of cleavage stage embryo mass (Gurdon and Wakefield, 1986; Baxi et al., 2019), and our metabolomic measurements were made on whole cell lysates (Onjiko et al., 2016). Yolk is the major source of amino acids, and yolk proteolysis, which could be the source of the metabolites detected in Onjiko et al. (2016) is regionally different during *Xenopus* early embryogenesis (Jorgensen et al., 2009). Although there is gradient of different sized yolk platelets along the animal-vegetal axis (Danilchik and Gerhart, 1987), very little yolk consumption was detected prior to midblastula stages (Jorgensen et al., 2009). A next important step will be to elucidate whether the L-R metabolite differences and changes in clone dispersal and gene expression we observed can be attributed to specific organelles including endoplasmic reticulum, Golgi bodies, mitochondria and/or yolk platelets.

ACKNOWLEDGEMENTS

We thank Martin Blum and Axel Schweickert (University of Hohenheim) for gifts of plasmids and many helpful discussions. We also thank Ali H. Brivanlou for the *dand5/coco* plasmid. This work was supported by the National Science Foundation under awards IOS-1832968 (P.N.) and DBI-1826932 (P.N. and S.A.M.) and the National Institutes of Health under awards R21 GM114854 (P.N.), R01 DE022065 (S.A.M) and R01 DE026434 (S.A.M). Xenbase (http://www.xenbase.org/, RRID: SCR_003280) and the National *Xenopus* Resource (http://mbl.edu/xenopus/, RRID: SCR_013731) provided critical resources. The authors do not have any conflicts of interest to declare.

Funding:

This work was supported by the National Science Foundation under awards IOS-1832968 (P.N.) and DBI-1826932 (P.N. and S.A.M.) and the National Institutes of Health under awards R21 GM114854 (P.N.), R01 DE022065 (S.A.M) and R01 DE026434 (S.A.M).

REFERENCES

Adams DS, Robinson KR, Fukumoto T, Yuan S, Albertson RC, Yelick P, Kuo L, McSweeney M, and Levin M. 2006. Early, H+-V-ATPase-dependent proton flux is necessary for consistent left-right patterning of non-mammalian vertebrates. Development 133: 1657–1671. [PubMed: 16554361]

Baxi A, Lombard-Banek C, Moody SA, Nemes P. 2018. Proteomic characterization of the neural ectoderm fated cell clones in the *Xenopus laevis* embryo by high-resolution mass spectrometry. ACS Chemical Neuroscience 9: 2064–2073. [PubMed: 29578674]

Blum M, Feistel K, Thumberger T. and Schweickert A. 2014. The evolution and conservation of left-right patterning mechanisms. Development 141: 1603–1613. [PubMed: 24715452]

Blum M and Ott T. 2018. Animal left-right asymmetry. Curr. Biol 28: R301–R304. [PubMed: 29614284]

Bunney TD, de Boer AH, and Levin M. 2003. Fusicoccin signaling reveals 14-3-3 protein function as a novel step in left-right patterning during amphibian embryogenesis. Development 130: 4847–4858. [PubMed: 12930777]

Chou HC, Pruitt MM, Bastin BR, and Schneider SQ. 2016. A transcriptional blueprint for a spiral-cleaving embryo. BMC Genomics 17: 552. [PubMed: 27496340]

Cofre J and Abdekhay E. 2007. Connexins in the early development of the African clawed frog *Xenopus laevis* (Amphibia): The role of the connexin43 carboxyl terminal tail in the establishment of the dorsal-ventral axis. Gen. Mole. Biol 30: 483–493.

Courtelis JB, Gonzalez-Morales N, Geminard C, and Noselli S. 2014. Diversity and convergence in the mechanisms establishing L/R asymmetry in metazoan. EMBO Rep. 15: 926–937. [PubMed: 25150102]

Danilchik MV, Brown EE, and Riegert K. 2006. Intrinsic chiral properties of the *Xenopus* egg cortex: an early indicator of left-right asymmetry? Development 133: 4517–4526. [PubMed: 17050623]

Danilchik MV, Gerhart JC. 1987. Differentiation of the animal-vegetal axis in *Xenopus laevis* oocytes. I. Polarized intracellular translocation of platelets establishes the yolk gradient. Dev. Biol 122: 101–112. [PubMed: 3596006]

Davidson EH. 1990. How embryos work: A comparative view of diverse modes of cell fate specification. Development 108: 365–389. [PubMed: 2187672]

De Domenico E, Owens ND, Grant IM, Gomes-Faria R, and Gilchrist MJ. 2015. Molecular asymmetry in the 8-cell stage *Xenopus tropicalis* embryo described by single blastomere transcript sequencing. Dev. Biol 408: 252–268. [PubMed: 26100918]

Gurdon JB, Wakefield L. 1986. Microinjection of amphibian oocytes and eggs for the analysis of transcription. In: Microinjections and Organelle Transplantation Techniques (ed. Celis JE, Graessmann A and Loyter A). London, Academic Press.

Heasman J 2006. Patterning the early *Xenopus* embryo. Development 133: 1205–1217. [PubMed: 16527985]

Hirose G and Jacobson M. 1979. Clonal organization of the central nervous system of the frog. I. Clones stemming from individual blastomere of the 16-cell and earlier stages. Dev. Biol 71: 191–202. [PubMed: 499655]

Houston DW. 2012. Cortical rotation and messenger RNA localization in *Xenopus* axis formation. Wiley Interdisc. Rev. Dev. Biol 1: 371–388.

Hyatt BA, Yost HJ. 1998. The left-right coordinator: the role of Vg1 in organizing left-right axis formation. Cell 93: 37–46. [PubMed: 9546390]

Jorgensen P, Steen JAJ, Steen H, Kirschner MW. 2009. The mechanism and pattern of yolk consumption provide insight into embryonic nutrition in *Xenopus*. Development 136: 1539–1548. [PubMed: 19363155]

Keller RE. 1975. Vital dye mapping of the gastrula and neurula of *Xenopus laevis*. I. Prospective areas and morphogenetic movements of the superficial layer. Dev. Biol 42: 222–241. [PubMed: 46836]

King ML, Messitt TJ, and Mowry KL. 2005. Putting RNAs in the right place at the right time: RNA localization in the frog oocyte. Biol. Cell 97:19–33. [PubMed: 15601255]

Kitaguchi T, Nagai T, Nakat K, Aruga J, and Mikoshiba K. 2000. *Zic3* is involved in the left-right specification of the *Xenopus* embryo. Development 127: 4787–4795. [PubMed: 11044394]

Klein SL. 1987. The first cleavage furrow demarcates the dorsal-ventral axis in *Xenopus* embryos. Dev. Biol 120: 299–304. [PubMed: 3817297]

Krejci A, and Tennessen JM. 2017. Metabolism in time and space – exploring the frontier of developmental biology. Development 144: 3193–3198. [PubMed: 28928279]

Kuroda R, Endo B, Abe M, and Shimuzi M. 2009. Chiral blastomere arrangement dictates zygotic left-right asymmetry pathway in snails. Nature 462: 790–794. [PubMed: 19940849]

Kuroda R, Fujikura K, Abe M, Hosoiri Y, Asakawa S, Shimizu M, Umeda S, Ichikawa F, and Takahasi H. 2016. Diaphanous gene mutation affects spiral cleavage and chirality in snails. Sci. Rep 6: 34809. [PubMed: 27708420]

Miyata S, Kageura H, and Kihara HK. 1987. Regional differences of proteins in isolated cells of early embryos of *Xenopus laevis*. Cell Diff. 21(1), 47–52

Moody SA. 1987. Fates of the blastomeres of the 16-cell stage *Xenopus* embryo. Dev. Biol 119: 560–578. [PubMed: 3803718]

Moody SA. 2018. Microinjection of mRNAs and oligonucleotides. Cold Spring Harbor Protocols. doi: 10.1101/pdb.prot097261.

Moody SA, and Kline MJ. 1990. Segregation of fate during cleavage of frog (*Xenopus laevis*) blastomeres. Anat. Embryol 182: 347–362.

Namigai EKO, Kenny NJ, and Shimeld SM. 2014. Right across the tree of life: The evolution of left–right asymmetry in the Bilateria. Genesis 52: 458–470. [PubMed: 24510729]

Nieuwkoop PD, and Faber F. 1994. Normal Table of *Xenopus laevis*. New York: Garland Publishing.

Onjiko RM, Moody SA, Nemes P. 2015. Single-cell mass spectrometry reveals small molecules that affect cell fates in the 16-cell embryo. Proc. Natl. Acad. Sci. USA 112: 6545–6550. [PubMed: 25941375]

Onjiko RM, Morris SE, Moody SA, Nemes P. 2016. Single-cell mass spectrometry with multi-solvent extraction identifies metabolic differences between left and right blastomeres in the 8-cell frog (*Xenopus*) embryo. Analyst 141: 3648–3656. [PubMed: 27004603]

Ramsdell AF, Bernanke JM, and Trisk TC. 2006. Left-right lineage analysis of the embryonic *Xenopus* heart reveals a novel framework linking congenital cardiac defects and laterality disease. Development 133: 1399–1410. [PubMed: 16527986]

Ryan AK, Blumberg B, Rodriguez-Esteban C, Yonei-Tamura S, Tamua T, de la Pena J, Sabbagh W, Greenwald J, Choe S, Norris DP, Robertson EJ, Evans RM, Rosenfeld MG and Izpisua Belmonte JC. 1998. Pitx2 determines left-right asymmetry of internal organs in vertebrates. Nature 394: 545–551. [PubMed: 9707115]

Schweickert A, Vick P, Getwan M, Weber T, Schneider I, Eberhardt M, Beyer T, Pachur A, Blum M. 2010. The nodal inhibitor Coco is a critical target of leftward flow in *Xenopus*. Curr. Biol 20: 738–743. [PubMed: 20381352]

Sempou E, Lakhani OA, Malraj S, and Khokha MK. 2018. Candidate heterotaxy gene FGFR4 is essential for patterning of the left-right organizer in *Xenopus*. Front. Physiol 04 Dec 2018: 10.3389/fphys.2018.01705

Stubbs JL, Oishi I, Izpisua Belmonte JC, and Kintner C. 2008. The forkhead protein Foxj1 specifies node-like cilia in *Xenopus* and zebrafish. Nat. Genet 40: 1454–1460. [PubMed: 19011629]

Tingler M, Ott T, Tözser J, Kurz S, Getwan M, Tisler M, Schweickert A, and Blum M. 2014. Symmetry breakage in the frog *Xenopus*: Role of Rab11 and the ventral-right blastomere. Genesis 52: 588–599. [PubMed: 24585437]

Vandenberg LN, Lemire JM, and Levin M. 2013. It's never too early to get it Right: A conserved role for the cytoskeleton in left-right asymmetry. Commun. Integr. Biol 6: e27155. [PubMed: 24505508]

Vastag L, Jorgensen P, Peshkin L, Wei R, Rabinowitz JD, Kirschner MW. 2011. Remodeling of the metabolome during early frog development. PLoS One e16881. doi: 10.1371/journal.pone.0016881. [PubMed: 21347444]

Vick P, Schweickert A, Weber T, Eberhardt M, Mencl S, Shcherbakov, Beyer T, and Blum M. 2009. Flow on the right side of the gastrocoele roof plate is dispensable for symmetry breaking in the frog *Xenopus laevis*. Dev. Biol 331: 281–291. [PubMed: 19450574]

Vonica A, and Brivanlou AH. 2007. The left-right axis is regulated by the interplay of Coco, Xnr1 and derriere in *Xenopus* embryos. Dev. Biol 303: 281–294. [PubMed: 17239842]

Warner AE, Guthrie SC, and Gilula N. 1984. Antibodies to gap-junctional protein selectively disrupt junctional communication in the early amphibian embryo. Nature 311: 127–131. [PubMed: 6088995]

Yan B, Neilson KM, and Moody SA. 2009. *foxD5* plays a critical upstream role in regulating neural ectodermal fate and the onset of neural differentiation. Dev. Biol 329: 80–95. [PubMed: 19250931]

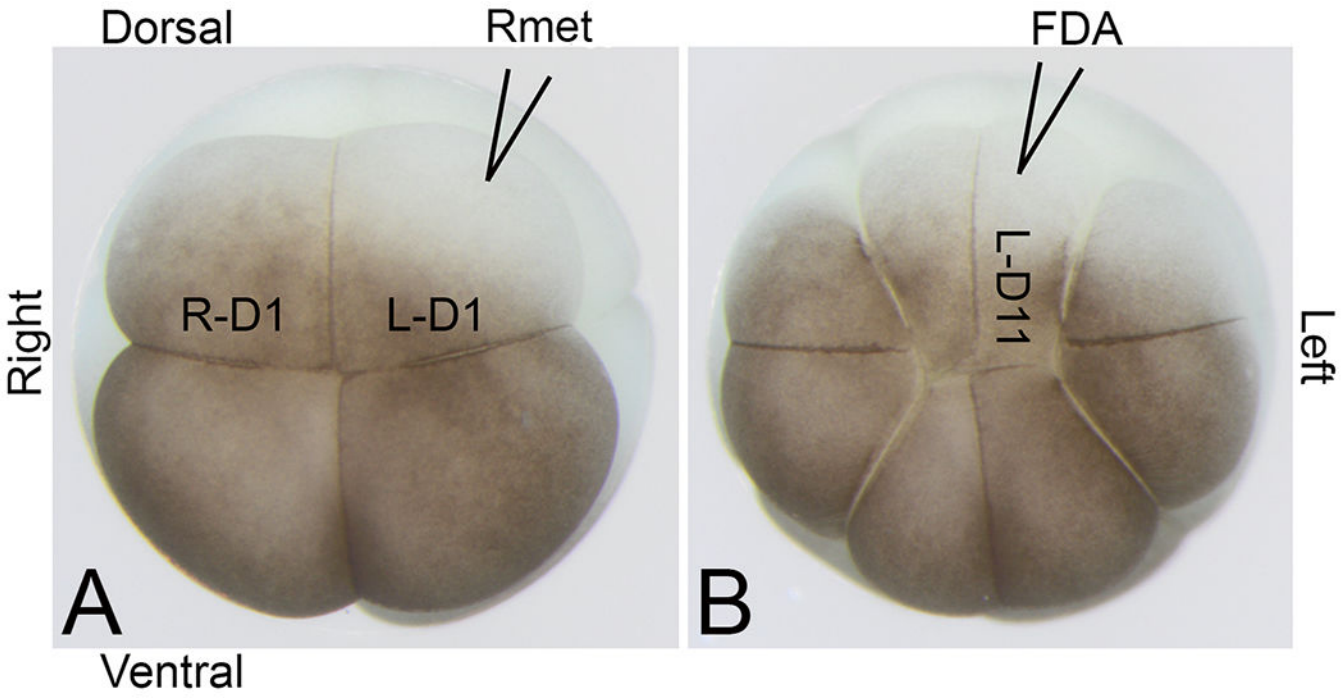

Figure 1:

Nomenclature of cleavage stage blastomeres (according to Hirose and Jacobson, 1979)

(A) Animal view of an 8-cell embryo with nomenclature of right dorsal-animal (R-D1) and left dorsal-animal (L-D1) blastomeres indicated. The cartoon of a micropipette filled with Rmet cocktail shows the microinjection strategy.

(B) Animal view of the same embryo at the 16-cell stage showing the midline descendant cell (L-D11) being microinjected with lineage tracer (fluorescein dextran amine, FDA) one cell division after the 8-cell mother blastomere (L-D1) was microinjected with Rmet cocktail.

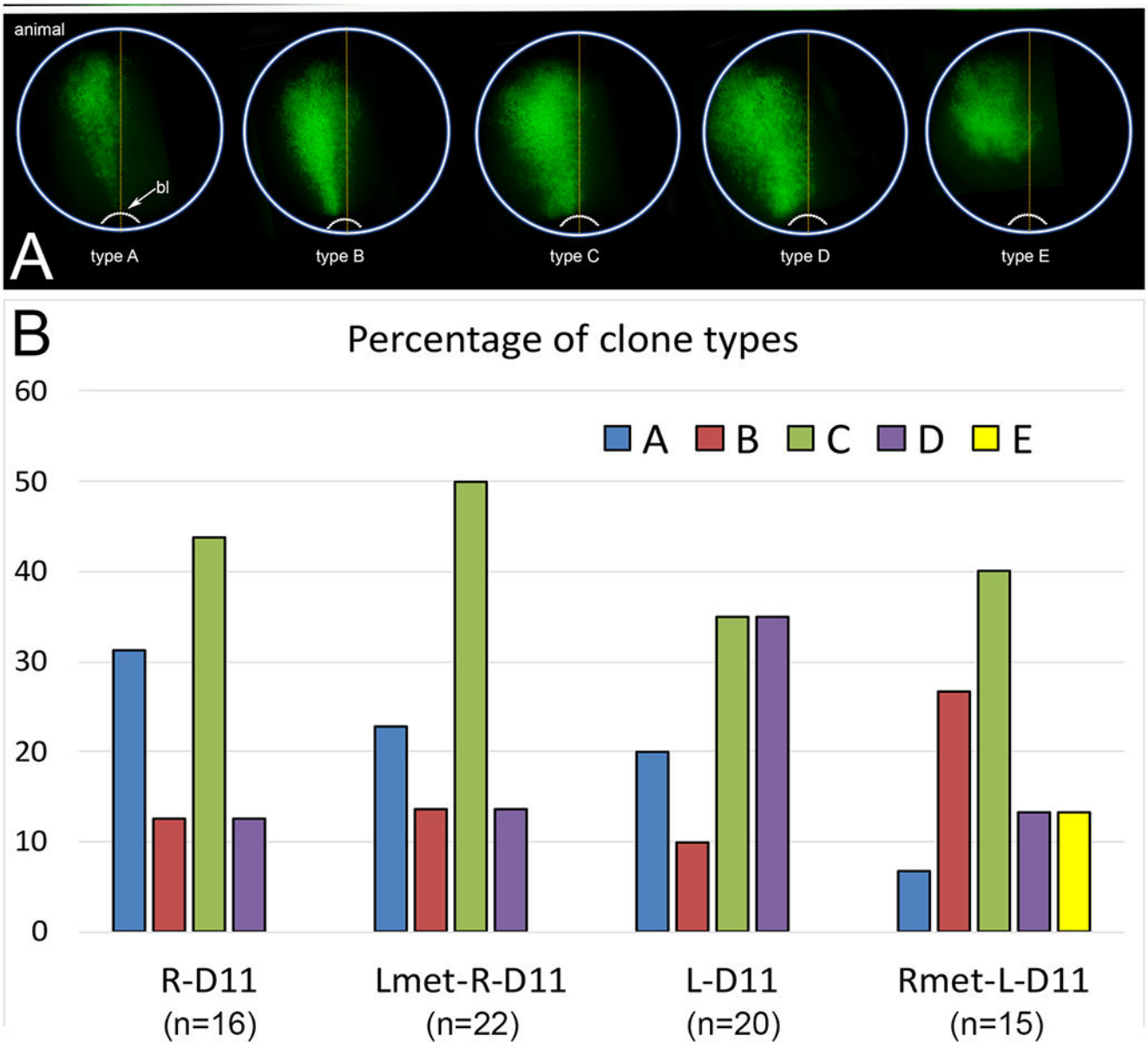

Figure 2:

Distribution patterns of FDA-labeled clones in the neural ectoderm at the end of gastrulation (stages 12-13).

(A) At the end of gastrulation, neural ectodermal clones of FDA-injected 16-cell dorsal midline blastomeres extended from the animal pole, which is the future forebrain region, to the posterior, closing blastopore (bl). The patterns were sorted into categories according to the lateral extent of the cells, from narrow (type A) to broad (type D), as described in the Methods. Type E was only observed in embryos in which the Rmet cocktail was injected into L-D1; it distinctly did not contain cells that extended to the blastopore.

(B) The frequency of the various types of clones observed for control embryos that were injected with only FDA, i.e., without added metabolites (R-D11, L-D11) or embryos

injected with metabolite cocktails at the 8-cell stage and then FDA at the 16-cell stage (Lmet-R-D11, Rmet-L-D11). Samples sizes are in parentheses.

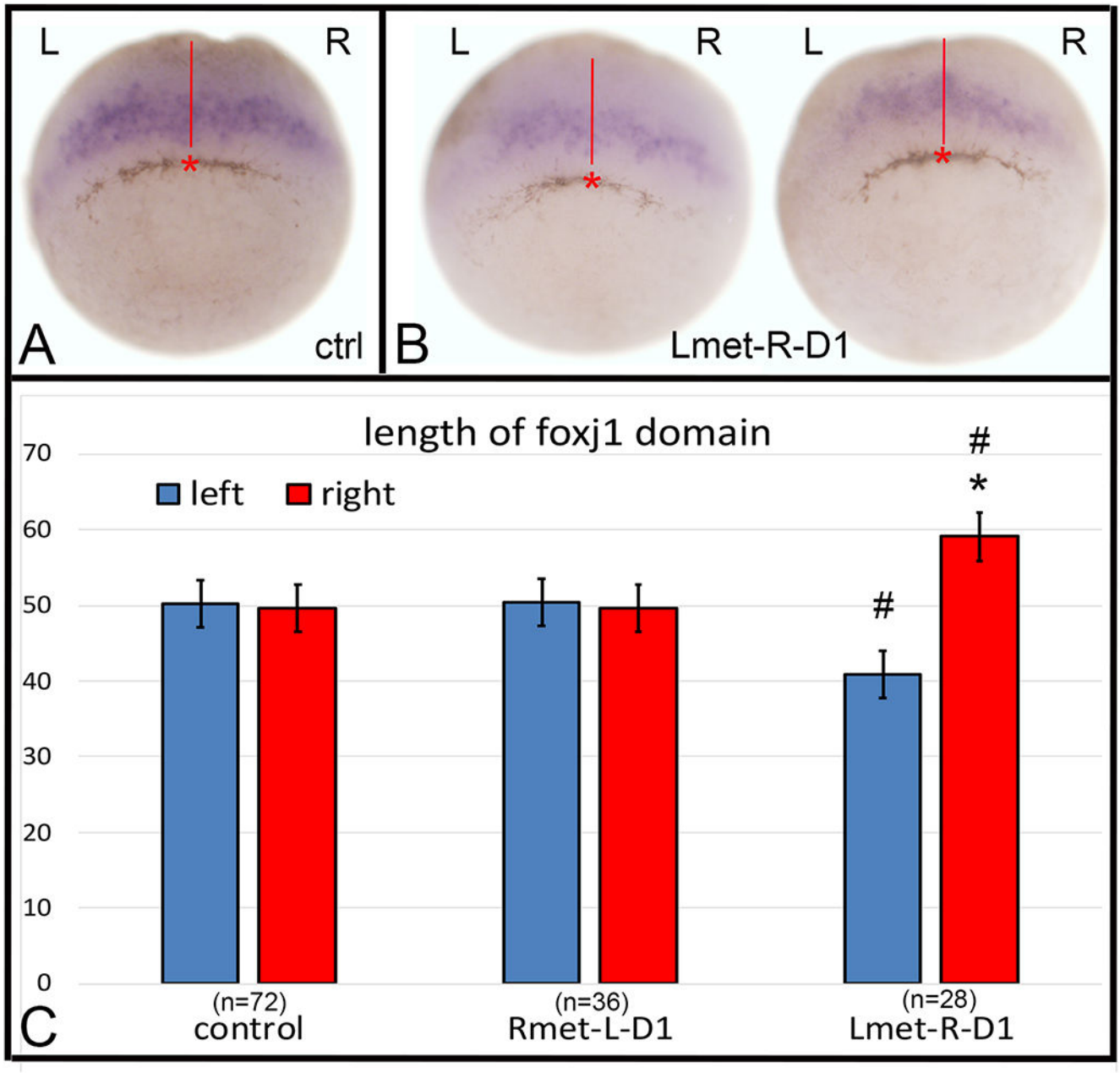

Figure 3:

Altering metabolite distributions at cleavage stages perturbs *foxj1* expression at gastrula stages.

(A) In control gastrula stage 10.5 embryos, *foxj1* expression (purple) was equivalent in length on the right (R) and left (L) sides of the embryo. Using a video camera attached to a stereomicroscope, the midpoint of the pigmented cells forming the blastopore, was marked (red asterisk), a line was drawn from that point towards the animal pole (red line) and the length of the *foxj1* expression domain measured from that line with an eyepiece reticule. **(B)** Examples of embryos in which the Lmet cocktail was injected into the R-D1 blastomere.

(C) Lengths of the right and left domains of *foxj1* expression in each embryo, in reticule units, were compared by a two-tailed, paired Wilcoxon test (* = $p < 0.005$). The right and left domains of *foxj1* expression in Lmet-R-D1 embryos were significantly different in length when compared by a two-tailed, paired Mann-Whitney test (# = $p < 0.0005$). Bars indicate SEM and samples sizes are in parentheses.

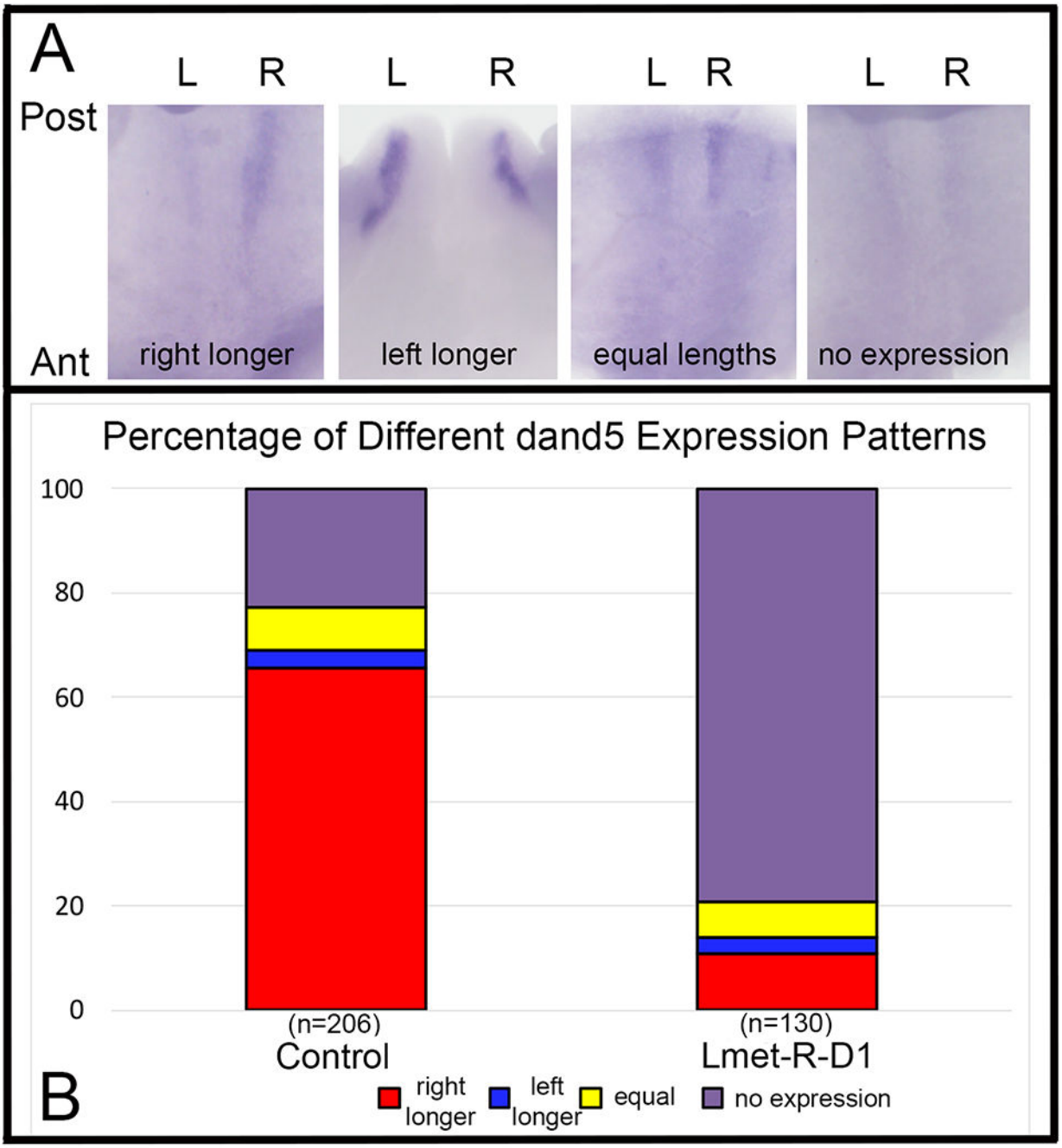

Figure 4:

Altered Lmet concentration in R-D1 perturbs *dand5* expression in the GRP.

(A) Expression of *dand5* in the GRP is typically larger, longer and/or darker on the right (R) side compared to the left (L) side (left panel), particularly in control embryos. In a minority of control cases, it was longer on the left side (left middle), equivalent in length on both sides (right middle) or not expressed at the stage examined (right panel). Tissue is oriented from a ventral view with posterior (Post) to the top and anterior (Ant) to the bottom.

(B) The frequencies of left-right *dand5* expression patterns were dramatically different between control embryos and siblings in which Lmet was injected into R-D1. Samples sizes are in parentheses.

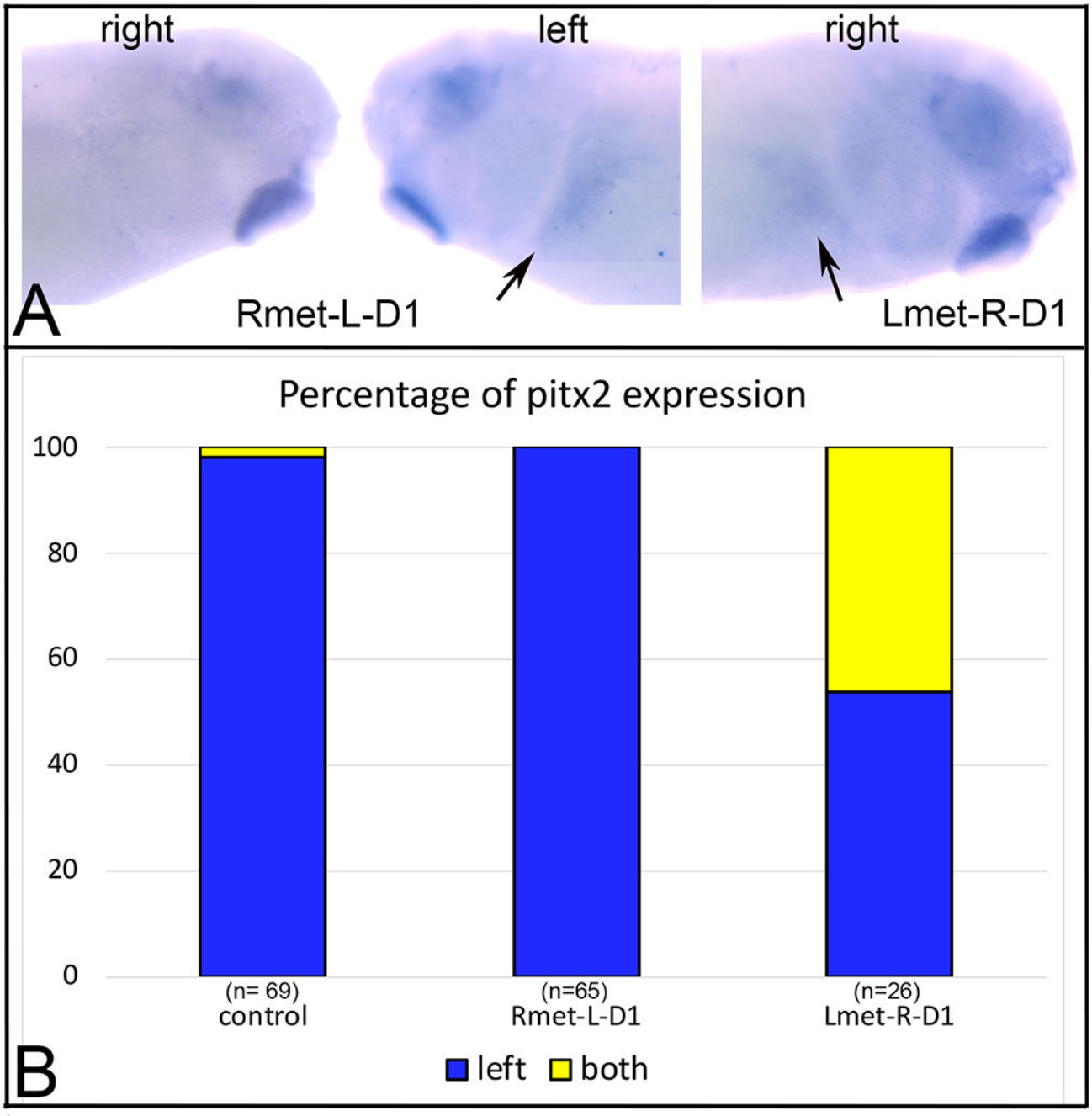

Figure 5:

Altering metabolite distribution on the right side at cleavage stages perturbs the distribution of *pitx2* expression in the larval lateral plate mesoderm.

(A) In an embryo in which Rmet cocktail was injected into L-D1, *pitx2* expression in the lateral plate mesoderm is confined to the left side (arrow).

(B) In an embryo in which Lmet cocktail was injected into R-D1, *pitx2* expression also was detected in the right lateral plate mesoderm (arrow). We did not observe any Lmet-R-D1 embryo in which *pitx2* was expressed only in the right lateral plate mesoderm.

(C) The percentage of embryos in which *pitx2* expression was detected on the left side or on both sides. Samples sizes are in parentheses.